Carbohydrate Polymers 87 (2012) 1596–1605

Contents lists available at SciVerse ScienceDirect

Carbohydrate Polymers

journal homepage: www.elsevier.com/locate/carbpol

Multifunctional bionanocomposite films of poly(lactic acid), cellulose nanocrystals and silver nanoparticles

E. Fortunati[a,*], I. Armentano[a], Q. Zhou[c,d], A. Iannoni[a], E. Saino[e,f], L. Visai[e,f,g,h], L.A. Berglund[d], J.M. Kenny[a,b]

[a] Materials Engineering Center, UdR INSTM, University of Perugia, Strada di Pentima 4, 05100 Terni, Italy
[b] Institute of Polymer Science and Technology, CSIC, Juan de la Cierva 3, 28006 Madrid, Spain
[c] School of Biotechnology, Royal Institute of Technology, SE-106 91 Stockholm, Sweden
[d] Wallenberg Wood Science Center, Royal Institute of Technology, SE-100 44 Stockholm, Sweden
[e] Department of Biochemistry, Medicine Section, Via Taramelli 3/B, 27100 Pavia, Italy
[f] Center for Tissue Engineering (C.I.T.), Via Ferrata 1, 27100 Pavia, Italy
[g] Salvatore Maugeri Foundation IRCCS, Via S. Maugeri 4, 27100 Pavia, Italy
[h] International Centre for Studies and Research in Biomedicine (ICB), 16 a, Bd. de la Foire, L-2015 Luxembourg

ARTICLE INFO

Article history:
Received 15 July 2011
Received in revised form 7 September 2011
Accepted 23 September 2011
Available online 29 September 2011

Keywords:
Polylactic acid
Nanocomposite
Nanocrystalline cellulose
Antibacterial response

ABSTRACT

Nanocomposite films were prepared by the addition of cellulose nanocrystals (CNCs) eventually surfactant modified (s-CNC) and silver (Ag) nanoparticles in the polylactic acid (PLA) matrix using melt extrusion followed by a film formation process. Multifunctional composite materials were investigated in terms of morphological, mechanical, thermal and antibacterial response. The nanocomposite films maintained the transparency properties of the PLA matrix. Thermal analysis showed increased values of crystallinity in the nanocomposites, more evident in the s-CNC based formulations that had the highest tensile Young modulus. The presence of surfactant favoured the dispersion of cellulose nanocrystals in the polymer matrix and the nucleation effect was remarkably enhanced. Moreover, an antibacterial activity against *Staphylococcus aureus* and *Escherichia coli* cells was detected for ternary systems, suggesting that these novel nanocomposites may offer good perspectives for food packaging applications which require an antibacterial effect constant over time.

1. Introduction

Packaging, including flexible films and rigid containers, is the largest single market for plastic material consumption and it is also one of the main sources of problems for post-consumption disposal of wastes. Biodegradable polymers have been investigated during the last few decades as alternatives to non-degradable polymers currently used in film production for different industrial applications (Bordes, Pollet, & Avérous, 2009; Davis & Song, 2006). In particular, poly(lactic acid) (PLA) is becoming increasingly popular as a biodegradable engineering plastic owing to its high mechanical strength and easy processability compared to other biopolymers. At present, due to its availability at relatively low prices in the market (Auras, Harte, & Selke, 2004), PLA has one of the highest potentials among biopolyesters, particularly for packaging and medical applications (Auras et al., 2004; Lunt, 1998). Demand for safe and minimally processed food products presents major challenges for the food-packaging industry to develop packaging concepts for maintaining the safety and quality of products. In this contest, the active food-packaging concepts provide some additional functions in comparison with traditional materials that are limited to protect food product against external influences. The incorporation of antimicrobial substances in food-packaging materials represents a promising way to synthesized active packaging materials and to control undesirable growth of microorganisms on the surface of foods (Vermeiren, Devlieghere, van Beest, de Kruijf, & Debevere, 1999). However, due to its deliberate interaction with the food and/or its environment active and intelligent packaging poses new challenges to the evaluation of its safety as compared to the traditional packaging. In this case the migration of substances from the packaging to food is the main risk while other risks could occur from the incorrect use of the packaging due to the insufficient labelling or the non-efficacious operation of the active packaging. Nowadays the introduction of new silver-filled antimicrobial polymeric materials represents a great challenge because the silver-based thermoplastic polymer composites combine the excellent processability of the thermoplastics with the inherent antimicrobial property of the silver (Morones et al., 2005; Williams, Doherty, Vince, Grashoff, & Williams, 1998). However, while the population exposed to silver nanoparticles continues to increase

* Corresponding author. Tel.: +39 0744 492921; fax: +39 0744 492950.
E-mail address: elena.fortunati@unipg.it (E. Fortunati).

0144-8617/$ – see front matter © 2011 Elsevier Ltd. All rights reserved.
doi:10.1016/j.carbpol.2011.09.066

with ever new applications, silver nanoparticles remain a controversial research area as regards their toxicity to biological systems. In particular, the oral toxicity of silver nanoparticles is of particular concern to ensure public and consumer health. Accordingly, Kim et al. (2008) tested the oral toxicity of silver nanoparticles over a period of 28 days in Sprague–Dawley rats. They proved that silver nanoparticles do not induce genetic toxicity in male and female rat bone marrow in vivo and the tissue distribution of silver nanoparticles did show a dose-dependent accumulation of silver content in all the tissues examined. Silver-based antimicrobials capture much attention not only because of the non-toxicity of the active Ag^+ to human cells (Williams et al., 1998) but also because of their novelty being a long lasting biocide with high temperature stability and low volatility.

In Japan, silver-substituted zeolite has been developed as the most common antimicrobial agent incorporated into plastics while on 9 June 2000 the AgION™ Silver Ion Technology received the approval of the Food and Drug Administration for use in all types of food-contact polymers in USA market (Quintavalla & Vicini, 2002). The EU-wide regulatory instruments covering antimicrobial substances differ distinctively in scope, depending upon both the intended application and the actual effect of the active substances. So far, it is not the active product itself, but its use conditions that determine which directive applies in regulating the marketing of food packaging products with antimicrobial activity in the European Union (Quintavalla & Vicini, 2002).

A new regulation of European Union (EU n. 10/2011 commission 14 January 2011) specific for packaging material, was published in 2011 and not particular indication for the use of silver compounds in packaging application was included. However, the use of some different metal particles, as titanium nanoparticles, started to be considered for these application fields.

The development of high performance nanocomposite films for packaging applications with polymer matrix and nanofillers that are fully renewable, represents a key point of the research. Cellulose nanocrystals (CNCs) have attracted significant attention during the last decade as potential nanoreinforcement in different polymers (Samir & Dufresne, 2005). Nanocrystalline cellulose, is typically a rigid rod-shaped monocrystalline domain with 1–100 nm in diameter and from tens to hundreds of nanometers in length depending on the resources of cellulose. CNCs have a crystalline structure, a very high aspect ratio (length/diameter around 70), and a large surface area (ca. 150 m^2/g) (Cavaille, Ruiz, Dufresne, Gerard, & Graillat, 2000). Cellulose nanocrystals can be produced from acid hydrolysis of various natural cellulose fibers such as cotton, cellulose fibers from lignocellulosic materials and a marine animal tunicate (Dong, Revol, & Gray, 1998; Edgar & Gray, 2002; Heux, Chauve, & Bonini, 2000). Therefore, CNC is commonly produced from the hydrolysis of microcrystalline cellulose (MCC) using sulphuric acid (Bondeson, Mathew, & Oksman, 2006) that removes the amorphous cellulose to form highly crystalline cellulose of colloidal dimensions with much smaller size than MCC. Cellulose nanocrystals have better mechanical properties than a majority of the commonly used reinforcing materials and offer additional exceptional advantages such as biodegradability and biocompatibility, high stiffness and low density. However, they also offer drawbacks due to the fact that nanocrystals have to be isolated and that their dispersion into the polymeric matrix has been shown to be problematic due to the low thermal stability, especially in extrusion processes (Oksman, Mathew, Bondeson, & Kvien, 2006). The possibility to use an acid phosphate ester of ethoxylated nonylphenol as a stabilizing agent, to obtain stable dispersions of CNC was previously reported (Bondeson et al., 2006; Bondeson and Oksman, 2007; Heux et al., 2000; Oksman et al., 2006).

In this research, melt compounding extrusion followed by a film forming process was explored as a technique of preparing cellulose nanocrystal based nanocomposites. For this purpose, PLA based high performance composites for packaging applications were produced using an innovative combination of nanocrystalline cellulose (CNC) and silver nanoparticles (Ag) in order to obtain multifunctional systems. Moreover, the CNC surface was modified using a surfactant (s-CNC) in order to increase the dispersion in PLA matrix. The goal of this study was to prepare binary and ternary nanocomposites with increased mechanical and thermal properties due to cellulose introduction, providing an antimicrobial response with the silver nanoparticles and to study the influence of nanodimensions and surfactant presence, on the dispersion of cellulose nanocrystals in the polymer matrix. Moreover, the influence of the combination of the cellulose structures with silver nanoparticles represents the novelty of the research.

2. Experimental

2.1. Materials

Poly(lactic acid) (PLA 3051D), with a specific gravity of 1.25 g/cm^3, a molecular weight (M_n) of ca. 1.42×10^4 g/mol, and a melt flow index (MFI) of 7.75 g/10 min (210 °C, 2.16 kg) was supplied by Nature Works®, USA. Commercial silver (Ag) nanopowder, P203, with a size distribution ranged from 20 to 80 nm, was purchased from Cima NanoTech (Corporate Headquarters Saint Paul, MN, USA). PLA pellets were dried in a vacuum oven at 98 °C for 3 h while Ag nanoparticles were thermal treated at 700 °C for 1 h (Fortunati, Armentano, Iannoni, & Kenny, 2010). Microcrystalline cellulose (MCC, dimensions of 10–15 μm) was supplied by Sigma–Aldrich.

2.2. Nanocrystal synthesis, modification and stability

Cellulose nanocrystal (CNC) suspension was prepared from MCC by sulphuric acid hydrolysis following the recipe used by Cranston and Gray (2006). Hydrolysis was carried out with 64% (w/w) sulphuric acid at 45 °C for 60 min with vigorous stirring. After removing the acid, dialysis, and ultrasonic treatment were performed. The resultant cellulose nanocrystal aqueous suspension was approximately 0.5% (w/w) by weight and the yield was ca. 20%. Mixed bed ion exchange resin (Dowex Marathon MR-3 hydrogen and hydroxide form) was added to the cellulose suspension for 48 h and then removed by filtration. This procedure ensured that all ionic materials were removed except the H^+ counter ions associated with the sulphate groups on the CNC surfaces. The nanocrystals were examined by transmission electron microscopy (TEM, Philips Tecnai 10) operated at an acceleration voltage of 80 kV. A droplet of dilute CNC suspension (0.1 wt%) was deposited on a bacitracin-pretreated surface of a carbon-coated grid.

Cellulose nanocrystals were modified with a surfactant, an acid phosphate ester of ethoxylated nonylphenol, in order to increase the dispersion in the polymer matrix and to enhance the final properties of nanocomposite systems. The CNC modified with surfactant (designed as s-CNC) was prepared by adding the Beycostat A B09 (CECCA S.A.) (Heux et al., 2000), to the suspension containing nanocrystals in portion of 1/1 (w/w).

The pH of pristine CNC suspension and s-CNC solution was around 3 at the end of preparation procedure. It was previously reported that such pH value corresponds to a very poor cellulose thermal stability (Petersson, Kvien, & Oksman, 2007). For this reason, the pH of cellulose nanocrystal suspensions, including pristine and surfactant modified, was raised to approximately 9 by the addition of 1.0% (w/w) of 0.25 mol/l NaOH. A thermogravimetric analysis (TGA, Seiko Exstar 6000) of CNC from suspensions without (pH 3) and with (pH 9) added NaOH was conducted in order to

Table 1
Material formulations.

Materials	PLA (wt%)	CNC (wt%)	s-CNC (wt%)	Ag (wt%)
PLA	100	–	–	–
PLA/5CNC	95	5	–	–
PLA/5s-CNC	95	–	5	–
PLA/5CNC/1Ag	94	5	–	1
PLA/5s-CNC/1Ag	94	–	5	1

evaluate the thermal stability with an isothermal test for 40 min, at the nanocomposite film process temperature of 185 °C.

The microstructure and agglomeration effects of unmodified and surfactant modified cellulose nanocrystals after the freeze-drying procedure were investigated by means of field emission scanning electron microscope (FESEM, Supra 25-Zeiss). Moreover, the thermal stability of freeze-dried nanocrystals was investigated by thermogravimetric analysis with a heating scan from 30 °C to 500 °C at 10 °C/min in a nitrogen atmosphere.

2.3. PLA nanocomposite processing

PLA nanocomposites were manufactured by using a twin-screw microextruder (DSM Explorer 5&15 CC Micro Compounder). Screw speed of 150 rpm and mixing time of 3 min were used in order to optimize material final properties, while a temperature profile of mixing process with a maximum kneading temperature of 185 °C was chosen in order to prevent the thermal degradation of both PLA and CNC.

Directly after the mixing process, a film forming process with a head force of 3000 N and a maximum temperature of 200 °C was performed in order to obtain PLA and PLA nanocomposite films with a thickness ranged from 20 to 80 μm. Binary nanocomposites with 5 wt% of pristine CNC or surfactant modified s-CNC and ternary nanocomposite films with 1 wt% of Ag and 5 wt% of CNC or s-CNC were also prepared and designed as PLA/5CNC, PLA/5s-CNC and PLA/5CNC/1Ag, PLA/5s-CNC/1Ag respectively. Cellulose nanocrystal and silver nanoparticle contents were selected on the basis of the our previous work (Fortunati et al., 2010) concerning microcrystalline cellulose and silver nanoparticles based multifunctional composites, in order to study the influence of nano-dimensions on the functional properties of the new cellulose nanocrystal based nanocomposites. The material formulations are shown in Table 1.

2.4. Characterization methods

Cross sections of the composites were sputtered with gold and analysed by FESEM, Supra 25-Zeiss. Microstructure of PLA nanocomposite films and filler dispersion in the matrix were investigated also by using transmission electron microscope (TEM, JEOL JEM-2010). Samples for TEM observations were previously ultramicrotomed (RMC, model MTXL) in order to obtain slices 100 nm thick.

The mechanical behaviour of neat PLA, binary and ternary PLA nanocomposite systems was evaluated by tensile tests, performed on rectangular probes (100 mm × 10 mm) on the basis of UNI ISO 527 with a crosshead speed of 5 mm/min, a load cell of 500 N and an initial gauge length of 50 mm. Average tensile strength (σ_b) and percentage elongation at break (ε_b %), yield stress and strain (σ_Y, ε_Y) and elastic modulus (E) were calculated from the resulting stress–strain curves. The measurements were done at room temperature and at least five samples were tested.

Thermogravimetric analysis (TGA, Seiko Exstar 6000) was performed on neat PLA and nanocomposite samples as follows: 10 mg weight samples, nitrogen (250 ml/min) or air (50 ml/min) flow, temperature range from 30 °C to 900 °C, heating rate of 10 °C/min. Thermal degradation temperatures (T_{max}) were evaluated.

Differential scanning calorimeter (DSC, Mettler Toledo 822/e) measurements were performed in the temperature range from −25 °C to 250 °C, at 10 °C/min, performing two heating and one cooling scans. Melting and cold crystallization temperatures and enthalpies (T_m, T_{cc} and ΔH_m, ΔH_{cc}) were determined from the first heating scan, while glass transition temperature (T_g) was measured from the heating and cooling scans. Crystallinity degree was calculated as:

$$\chi = \frac{1}{1 - m_f}\left[\frac{\Delta H_m - \Delta H_{cc}}{\Delta H_{m0}}\right] \times 100 \quad (1)$$

ΔH_m is the enthalpy for melting, ΔH_{m0} is enthalpy of melting for a 100% crystalline PLA sample, taken as 93 J/g (Riga, Zhang, & Collis, 2004) and $(1 - m_f)$ is the weight fraction of PLA in the sample.

2.5. Antibacterial activity

In this study the microorganisms used were *Escherichia coli* RB (*E. coli* RB), provided by Dr. Roldano Bragoni (Zooprofilattico Institute of Pavia, Italy), and *Staphylococcus aureus* 8325-4 (*S. aureus* 8325-4), a gift from Timothy J. Foster (Department of Microbiology, Dublin, Ireland). *E. coli* RB was grown overnight in Luria Bertani Broth (LB) (Difco, Detroit, MI, USA) and *S. aureus* 8325-4 in Brain Heart Infusion (BHI) (Difco) under aerobic conditions at 37 °C using a shaker incubator (New Brunswick Scientific Co., Edison, NJ, USA). These cultures, used as source for the experiments, were reduced at a final density of 1×10^{10} cells/ml as determined by comparing the OD_{600} of the sample with a standard curve relating OD_{600} to the cell number. To evaluate the antimicrobial activity of PLA and PLA nanocomposite films, 100 μl (1×10^4) of an overnight diluted cell suspension of *E. coli* RB or *S. aureus* 8325-4 was added to each sample and incubated at different temperatures (37 °C, 24 °C and 4 °C) for 3 h and 24 h, respectively. The selected temperatures were chosen to evaluate the influence of temperature on the antibacterial activity efficiency exerted by PLA nanocomposites as food packaging: some food is usually kept refrigerated at +4 °C but it may be possible that under transportation food is more likely kept at higher temperature of storage (24 °C and/or 37 °C). Furthermore, 24-well flat-bottom sterile polystyrene culture plates (TCP) used as controls were incubated for the same temperatures and times. At the end of each incubation time, the bacterial suspension was then serially diluted, and plated on the LB (*E. coli*) or BHI (*S. aureus*) agar plates, respectively. The plates were then incubated for 24 h at 37 °C. Cell survival was expressed as percentage of the CFU of bacteria grown on the materials samples to CFU of bacteria grown into 24-well TCP.

3. Results

3.1. Cellulose nanocrystals

Fig. 1 shows a TEM image of cellulose nanocrystals. The CNCs are individualized with typical dimensions ranging from 100 to 200 nm in length and 5–10 nm in width (Kvien, Tanem, & Oksman, 2005; Petersson et al., 2007). Thermogravimetric analysis (Fig. 2) of freeze-dried CNC from suspensions without (pH 3) and with (pH 9) added NaOH, conducted at the extrusion process temperature of 185 °C, shows a clear improvement of the thermal stability for the neutralized crystals (pH 9), in which the H^+ counter ions associated with the sulphate groups were interchanged with Na^+ on the nanocrystals surface.

Prior to the extrusion process, the CNC suspension was freeze-dried, in order to dry-mix them together with the polymer. During this process CNC reveals their natural tendency to re-agglomerate and form strong hydrogen bonds as the water sublimate. Fig. 3a and b shows freeze-dried CNC from a water suspension without

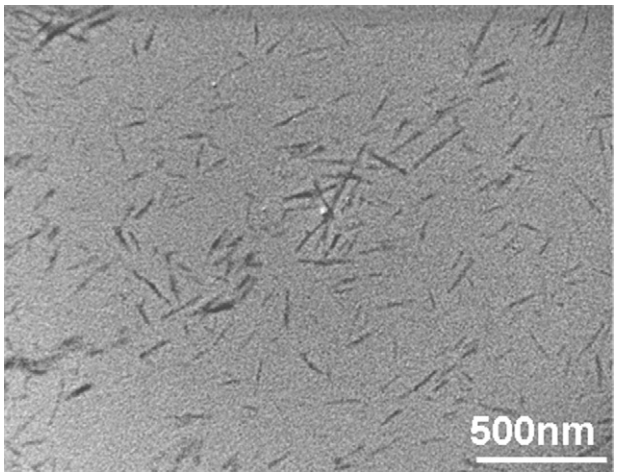

Fig. 1. TEM analysis of cellulose nanocrystal suspensions.

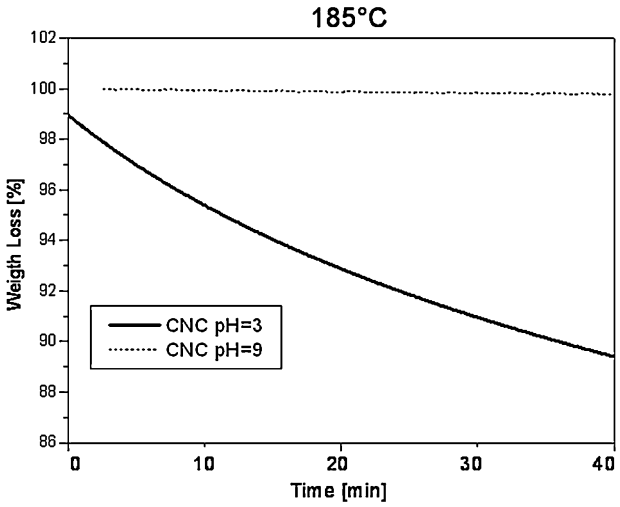

Fig. 2. Thermogravimetric analysis at 185 °C from suspensions without (pH 3) and with (pH 9) added NaOH.

surfactant. The nanocrystals are not isolated but agglomerated into flakes due to strong hydrogen bonds formation as the water sublimate during the freeze-drying. This freeze-drying step is critical for the production of nanocomposites with uniform CNC dispersion. Therefore, one possible solution to avoid agglomeration would be to use a surfactant that will cover the CNC and thereby hinder the nanocrystals from agglomeration. Fig. 3c and d shows freeze-dried s-CNC from a water suspension, and no crystal flakes appear but the isolated acicular structures typical of CNC (Fig. 1) are evident. TGA results are reported in Fig. 4, which shows residual weight vs. temperature (TG) and the derivative curves (DTG) for commercial microcrystalline cellulose powder (MCC), pristine and surfactant modified nanocrystalline cellulose. A slight decrease in weight for all materials below 150 °C is evident which was due to the moisture content of these materials. MCC showed the typical decomposition (Lu & Hsieh, 2010) with onset temperature just above 300 °C followed by a massive loss leaving only 7.9% ash at 500 °C (Fig. 4a). The cellulose nanocrystals, showed a more gradual thermal transitions that started at a lower temperature around 150–250 °C (initial degradation temperatures at 230 °C for unmodified CNC). Pristine CNC lost nearly 50% of their mass in the 150–300 °C region followed by another 25% mass loss between 300 and 500 °C, leaving significantly higher residue, nearly 23%, at 500 °C. These major thermal differences between the cellulose nanocrystals and the original cellulose powders may involve different decomposition/gasification processes, likely due to the acid hydrolysis used to produce the crystals. The gradual mass loss of the cellulose nanocrystals in the 150–300 °C temperature range suggests a different decomposition mechanism, possibly direct solid-to-gas phase transitions catalyzed by sulphate groups on the surface. In fact, it has been reported that the activation energies of the cellulose nanocrystal degradation were significantly lowered by introducing sulphate groups via sulphuric acid hydrolysis (Roman & Winter, 2004). On the other hand, the surfactant modified s-CNC appears more stable than the pristine CNC with a lower weight loss value in the region

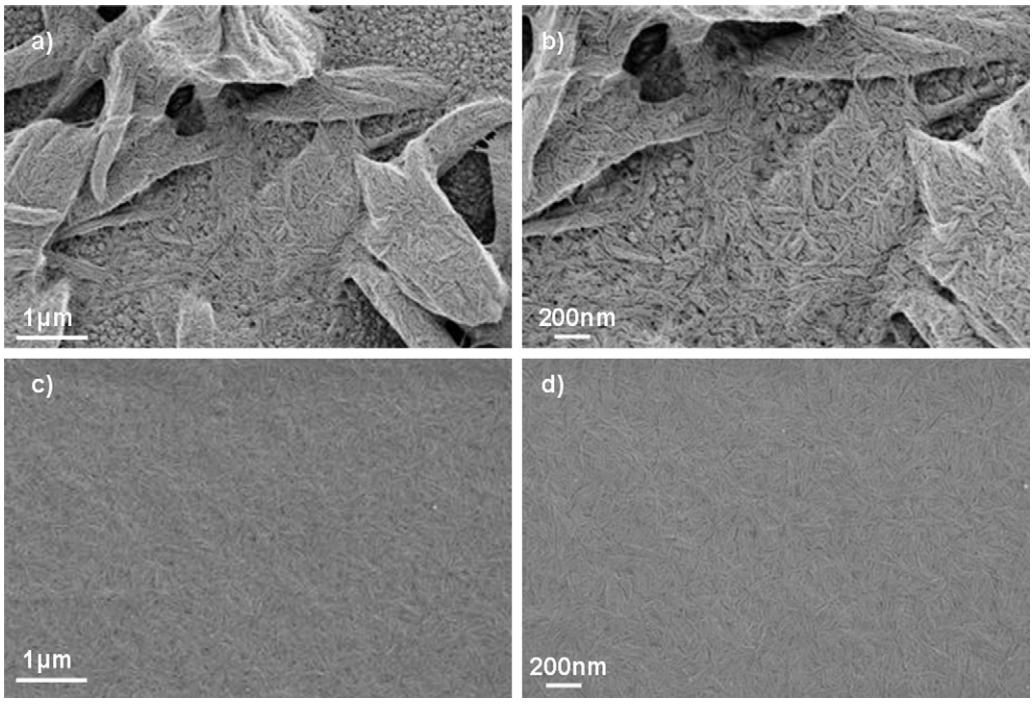

Fig. 3. Microstructure of freeze-dried cellulose nanocrystals without surfactant (a and b) and with surfactant (c and d).

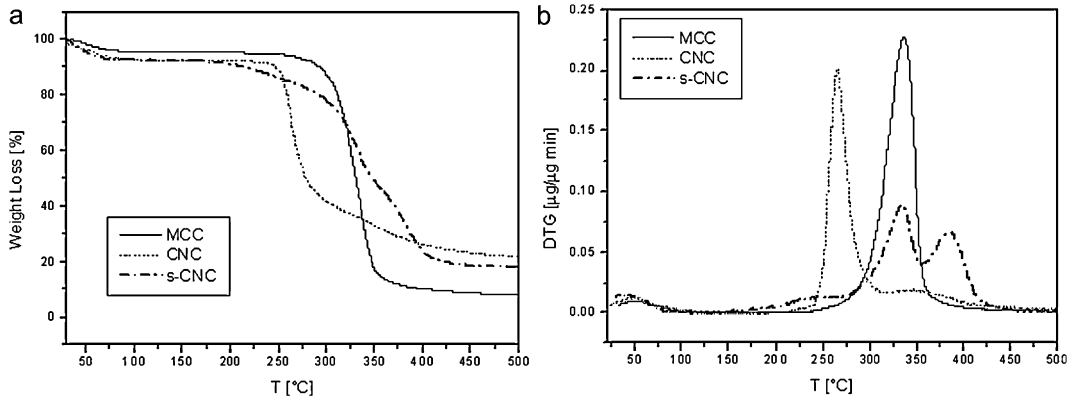

Fig. 4. TG (a) and DTG (b) curves of different cellulose structures.

between 150 and 300 °C (initial degradation temperatures at 200 °C for surfactant modified s-CNC) and Fig. 4b clearly shows that the weight loss of s-CNC occurs more stepwise than for the other materials between 300 and 500 °C (Petersson et al., 2007; Wang, Ding, & Cheng, 2007). TGA thermograms also underline that all materials were substantially thermally stable in the region below 200 °C. The recommended processing temperature of PLA is 190–200 °C and all the considered cellulose structures were able to maintain more than 93% of their original weight below this temperature.

3.2. Morphological analysis of PLA nanocomposites

Fig. 5 shows a photograph of PLA nanocomposite films. The nanocomposite systems maintained the transparency properties of the PLA matrix. However, binary and ternary systems containing s-CNC, appear more transparent than the systems with pristine CNC that showed a reduction of the transparency due to their dispersion in polymer matrix (Petersson & Oksman, 2006).

The fracture surfaces of PLA binary and ternary nanocomposites were investigated by FESEM (Fig. 6) in order to evaluate the influence of cellulose nanocrystal and silver nanoparticle introduction on the microstructure. In PLA/5CNC (Fig. 6a) nanocrystals appear agglomerated in the PLA matrix and some flakes are evident. These CNC flakes are formed during the freeze-drying process and the shear force during the extrusion is not enough to disperse them. Surface fracture of the PLA/5s-CNC (Fig. 6b) shows some s-CNC flakes embedded in the PLA matrix, however they present a smaller dimension than the CNC and a better distribution is detected for this system due to surfactant introduction. FESEM investigations were

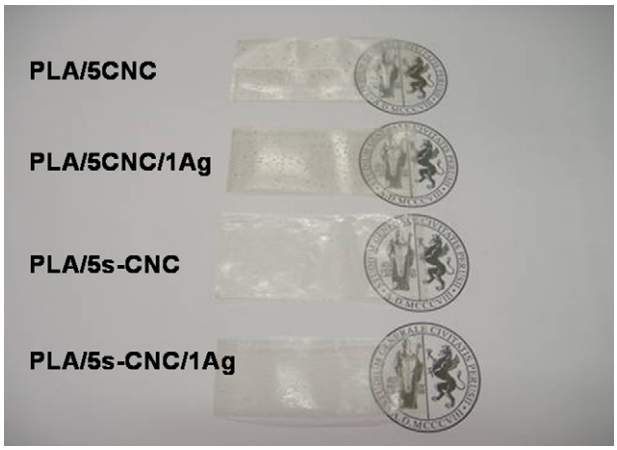

Fig. 5. Image of PLA nanocomposites.

also conducted on fractured surfaces of PLA ternary nanocomposites. Fig. 6c and d shows the PLA/5CNC/1Ag nanocomposite and, as in the case of binary system, CNC flakes appear embedded in the PLA matrix (arrows). The shape and the dimensions of CNC agglomerates induce different nanocomposite surface morphology respect to the s-CNC based ternary system (Fig. 6e and f), as a consequence of a combination of a different production process and the surfactant presence. The cellulose nanocrystals, in fact, have been able to separate from each other forming looser and smaller agglomerates compared to the PLA/5CNC/1Ag system with pristine nanocrystals. Moreover, an increase of surface roughness is evident for the ternary composite with s-CNC, no detected for the unmodified system, maybe due to the combining presence of silver nanoparticles (see insert) and, in large part, of surfactant presence (Bondeson and Oksman, 2007).

Fig. 7 shows the morphology and nanostructure dispersion of the binary and ternary composite films analysed by TEM. For the binary (PLA/5CNC) and ternary system (PLA/5CNC/1Ag) based on pristine nanocrystals (Fig. 7a and c respectively) it was found that the majority of the cellulose crystals were present in flakes. Fig. 7c (insert) shows a cross-section of a flake in the PLA matrix that consisted of tightly packed cellulose nanocrystals. In the s-CNC based nanocomposites it was possible to detect looser agglomerates of nanocrystals evident for both binary PLA/5s-CNC and ternary PLA/5s-CNC/1Ag systems (Fig. 7b and d). This indicates that the loosely bonded network created using the surfactant during the freeze drying process allowed the PLA chains to penetrate in between the cellulose structures. However, in the TEM images it was difficult to identify single crystals because of low contrast between PLA and cellulose structures. The same problem had been experienced by other researchers (Bondeson, Syre, & Oksman, 2007) and it is remarkably evident in s-CNC based systems due to the better dispersion of these cellulose structures since the pristine CNC agglomerate received better contrast in the TEM analysis. Fig. 7d shows a uniform morphology of the ternary s-CNC based system with a small flake of crystals in which in possible to see also an agglomeration of silver nanoparticles that tend to accumulate on the cellulose surface (see insert).

3.3. Mechanical characterization of PLA nanocomposites

The mechanical behaviour of neat PLA and PLA nanocomposites was evaluated and tensile test results are reported in Table 2. Values of binary PLA/1Ag systems obtained previously (Fortunati et al., 2010) are also reported for comparison. All studied nanocomposite formulations showed Young modulus higher than neat PLA (2.4 GPa), but the highest increase was detected for the binary PLA/5s-CNC nanocomposite (83%). An increase of 25% respect to

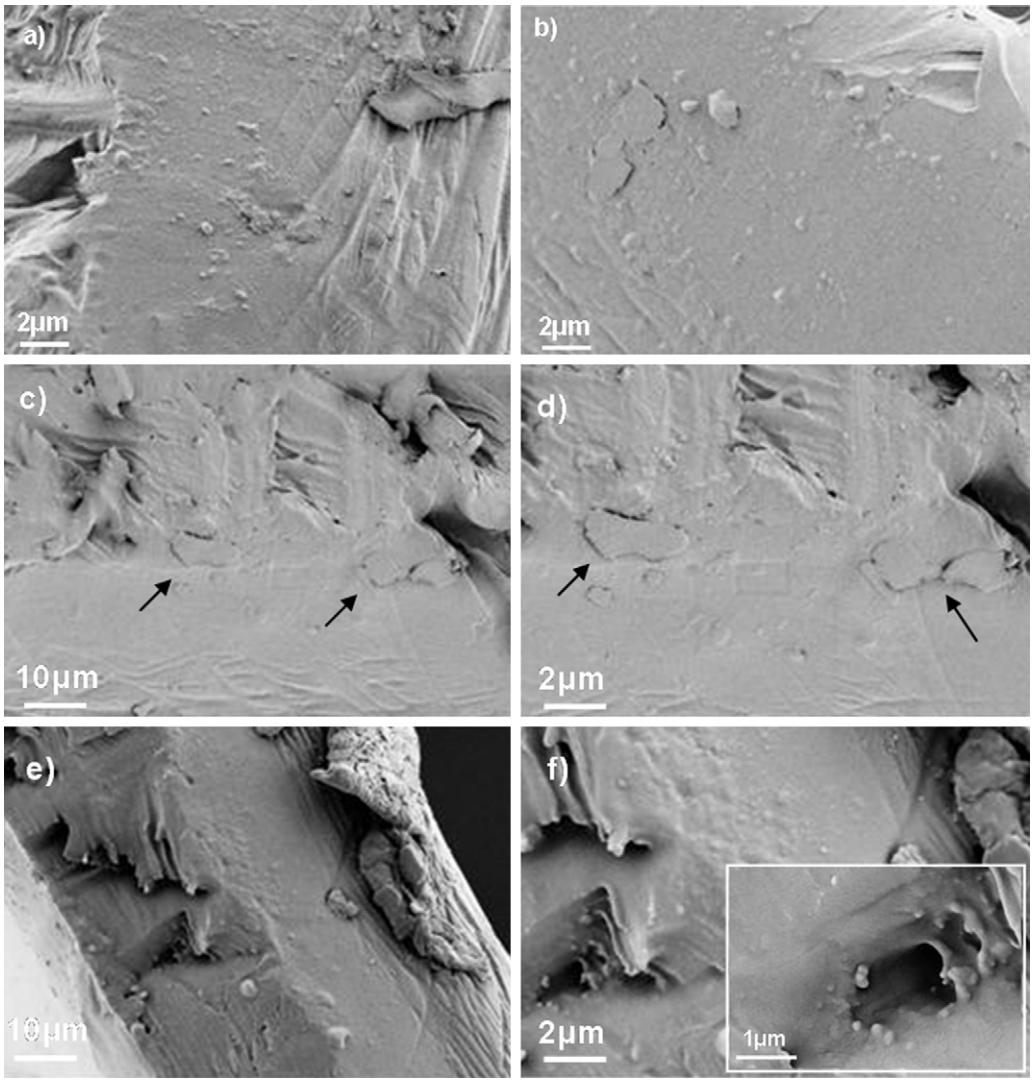

Fig. 6. Microstructure of fracture surface of PLA/5CNC (a) and PLA/5s-CNC (b) binary systems and of PLA/5CNC/1Ag (c and d) and PLA/5s-CNC/1Ag (e and f) ternary systems.

PLA polymer matrix, was detected also in the case of PLA/5s-CNC/1Ag ternary systems. These results highlight the effect of reinforcement exerted by CNC especially the modified s-CNC, and the efficiency of the surfactant on the dispersion of the cellulose nanostructures. This result was also confirmed by tensile at break values. Tensile strength is lower in the nanocomposites with pristine CNC compared to pure PLA film (Bondeson and Oksman, 2007). However, a different behaviour was detected for the s-CNC based systems, both binary and ternary ones, that present tensile strength values comparable with respect to the polymer matrix. The surfactant modification allowed a better nanocrystals dispersion with a consequent improvement of tensile strength in the nanocomposites. Moreover, a decrease of the PLA composite elongation at break respect to the PLA matrix for CNC and s-CNC based systems is detected. The lowering of elongation at break with the addition of fibers in the polymers, is a common trend observed in thermoplastic composites. The elongation at break is affected by the volume fraction of the added reinforcement, the dispersion in the matrix, and the interaction between the reinforcement and the matrix (Colom, Carrasco, Pages, & Canavate, 2003). In our case, cellulose nanocrystals cause substantial local stress concentrations and then failure at reduced strain values. In addition, although the modification of cellulose nanocrystals improved their dispersion degree, probably the interfacial adhesion between PLA and cellulose nanocrystals was not enhanced (Pei, Zhou, & Berglund, 2010). However, an higher value of elongation at break (60%) was maintained for PLA/5s-CNC/1Ag due to the combination of s-CNC with silver nanoparticles. The dispersion of the nanocrystals inside the

Table 2
Results from tensile test for PLA nanocomposite films.

Samples	σ_Y [MPa]	ε_Y [%]	σ_b [MPa]	ε_b [%]	E_{Young} [MPa]
PLA	54 ± 5	2.2 ± 0.5	43.0 ± 5.0	90 ± 10	2400 ± 100
PLA/1Ag	31 ± 3	2.1 ± 0.5	22.0 ± 3.0	11 ± 2	2520 ± 50
PLA/5CNC	39 ± 1	2.3 ± 0.2	28.3 ± 0.6	36 ± 1	2930 ± 20
PLA/5CNC/1Ag	48 ± 2	2.1 ± 0.1	29.0 ± 2.0	27 ± 5	2700 ± 100
PLA/5s-CNC	54 ± 5	1.2 ± 0.1	46.1 ± 3.0	18 ± 1	4400 ± 200
PLA/5s-CNC/1Ag	54 ± 5	1.9 ± 0.1	40.8 ± 3.0	60 ± 5	3000 ± 200

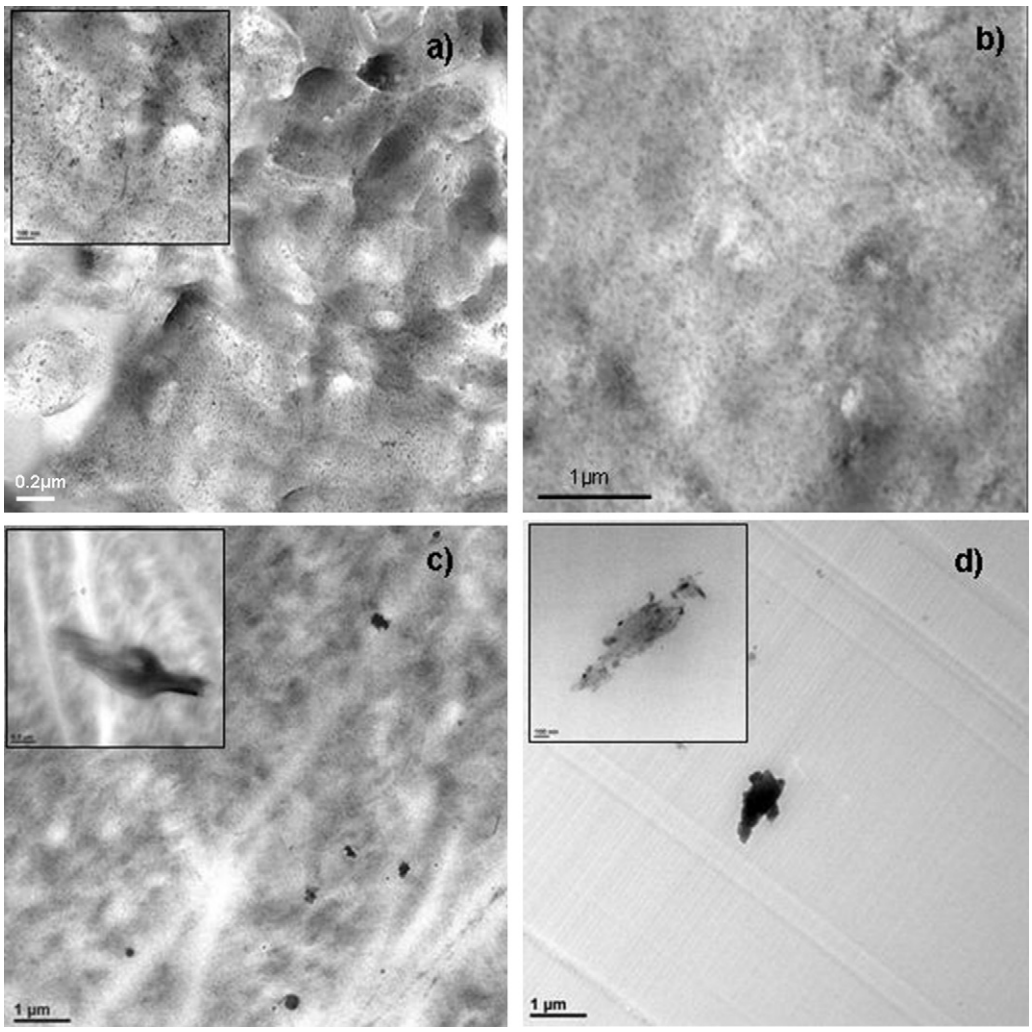

Fig. 7. TEM images of PLA/5CNC (a) and PLA/5s-CNC (b) binary systems and of PLA/5CNC/1Ag (c) and PLA/5s-CNC/1Ag (d) ternary systems.

matrix, and the surfactant ability to cover the crystals and to promote a direct interaction between the PLA, is of great importance since it governed the available surface area of cellulose as previously reported for binary cellulose composites (Bondeson and Oksman, 2007). The results obtained for nanocomposite mechanical behaviour in the plastic region, are a critical point for their employment in the industrial packaging field where a high elongation at break combined to an increment in tear resistance are request (Martino, Ruseckaite, & Jiménez, 2006). However, polymers films for packaging have a wider range of requirements from some units % to values higher than 200% of elongation at break depending on the specific sector of applications (from flexible films for meats to more rigid films for vegetables, bread and pasta). Further studies are needed to improve these trends, allowing to maintain high modulus values and, at the same time, obtaining high performance in plastic region. Lower content of cellulose structures (i.e. 1 wt%), chemical modification at the interface between PLA polymer matrix and the reinforcement phases, and/or the employment of plasticizer during the production process, could be possible strategies in order to involve these multifunctional materials in industrial applications.

3.4. Thermal behaviour of PLA nanocomposites

One of the goals of incorporating nanocrystals into PLA matrix is to increase the temperature region where the polymer can be processed and used. For this reason, the thermal properties of nanocomposite systems were also evaluated by means of thermogravimetric analysis performed in nitrogen and oxidative atmosphere. The weight loss (TG) and derivate DTG curves of binary and ternary nanocomposites are reported in Fig. 8. All the systems tested in nitrogen atmosphere show the same behaviour with a main degradation peak that starts around 300 °C and has its maximum at 357 °C for PLA matrix and the nanocomposite with s-CNC (Fig. 8a), and at around 360 °C for the system with pristine CNC (Fig. 8b). On the whole, TGA showed that there was no degradation taking place in both nanocrystal based composites in the temperature region (25–220 °C) where PLA is either processed or used.

PLA matrix degradation is scarcely influenced by the presence of oxidative flow and the degradation temperatures in nitrogen and air fall in the same range of temperature (Fig. 8c and d). PLA matrix shows a maximum degradation peak of 364 °C as previously reported for this grade of polymer (Ha & Xanthos, 2010). However, a similar trend respect to nitrogen atmosphere was detected for s-CNC based nanocomposites with a maximum degradation temperature at around 358 °C and a broader peak (Fig. 8c) respect to for PLA matrix. The presence of pristine CNC promotes an increase of the T_{max} of about 5–8 °C more evident in the case of binary system (Fig. 8d). Moreover, the mass loss curves for ternary systems (Fig. 8c and d inserts) highlight a residual mass of 1% related to the presence of silver nanoparticles.

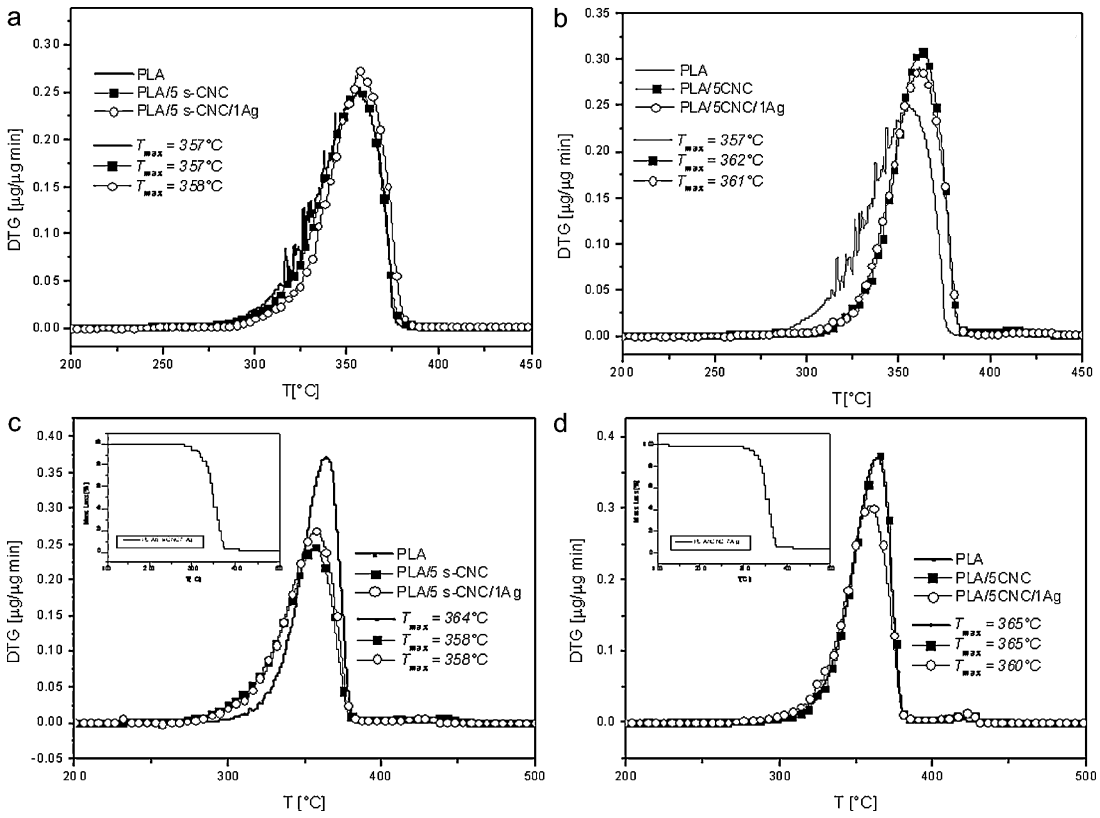

Fig. 8. DTG curves of PLA and PLA binary and ternary films loaded with s-CNC (a and c) and CNC (b and d) under nitrogen and air respectively. The inserts show the mass loss under air for PLA/5s-CNC/1Ag (c) and PLA/5CNC/1Ag (d) ternary systems.

Differential scanning calorimetry was used to investigate the glass transition, crystallization and melting phenomena of PLA and PLA nanocomposites. DSC thermal properties are summarized in Table 3. The glass transition temperatures of the nanocomposites do not change significantly respect to the polymer matrix. The T_g values, at the first heating scan, change to almost 5 °C with sample composition respect to PLA matrix and no significant differences for the unmodified CNC and surfactant modified s-CNC based nanocomposites were detected. Moreover, the results for nanocomposites reveal a reduction in the cold crystallization temperature, more evident in the case of ternary systems with a shift to lower temperature in the order of 10 °C. The ability to re-crystallize increased in filled PLA especially in the case of s-CNC based composites. The neat PLA film shows a 9.2% (Liao, Yang, Yu, & Zhou, 2007) crystallinity degree which is raised up to 18% in PLA/5s-CNC/1Ag ternary systems and reached 20% for binary PLA/5s-CNC. The presence of surfactant on the nanocrystal surface, favours the dispersion of the filler in the polymer matrix and the nucleation effect was remarkably enhanced when a more homogeneous s-CNC dispersion was achieved.

These results are in agreement with the mechanical properties that highlighted an increase of the elastic modulus value for nanocomposite resulting from more efficient dispersion and alignment of the functionalized nanocrystals (s-CNC) as shown in FESEM analysis.

3.5. Antibacterial properties

Fig. 9 shows the viability of *S. aureus* (panels A and B) and *E. coli* (panels C and D) cells onto PLA and PLA nanocomposite films after 3 h and 24 h incubation at 4 °C, 24 °C or 37 °C, respectively. A significant difference in viability for both bacterial strains between PLA and PLA nanocomposite films ($p < 0.05$) was observed at each time and for the temperatures indicated. In general PLA nanocomposites showed an antibacterial activity but with some differences. The antibacterial activity was more significant on PLA/5CNC/1Ag and PLA/5s-CNC/1Ag if compared with PLA/5CNC and PLA/5s-CNC ($p < 0.05$). These data are confirmed by previous reports showing that silver ions, interfering with the respiratory chain, can cause a decrease of the bacterial viability (Rai, Yadav, & Gade, 2009).

Table 3
Thermal properties of PLA and PLA nanocomposites at the first heating scan.

Samples		Cold crystallization		Melting		Crystallinity
	T_g [°C]	T_{cc} [°C]	ΔH_{cc} [J/g]	T_m [°C]	ΔH_m [J/g]	x [%]
PLA	59.0 ± 0.5	122.0 ± 0.6	7.5 ± 0.2	155.0 ± 1.9	16.1 ± 0.3	9.2 ± 0.2
PLA/1Ag	56.0 ± 0.4	119.2 ± 0.6	10.0 ± 0.5	149.4 ± 0.2	21.0 ± 0.3	12.0 ± 0.6
PLA/5CNC	54.6 ± 0.2	117.4 ± 1.0	15.2 ± 1.0	149.3 ± 0.2	25.7 ± 1.0	11.8 ± 0.8
PLA/5CNC/1Ag	54.7 ± 0.4	116.2 ± 0.7	14.1 ± 0.6	148.7 ± 0.2	19.7 ± 1.0	6.4 ± 0.9
PLA/5s-CNC	54.2 ± 0.3	110.3 ± 0.5	21.9 ± 0.2	148.4 ± 0.6	38.2 ± 0.2	18.5 ± 0.5
PLA/5s-CNC/1Ag	54.1 ± 0.6	112.4 ± 0.6	17.4 ± 0.5	149.7 ± 0.7	33.0 ± 0.4	17.7 ± 0.2

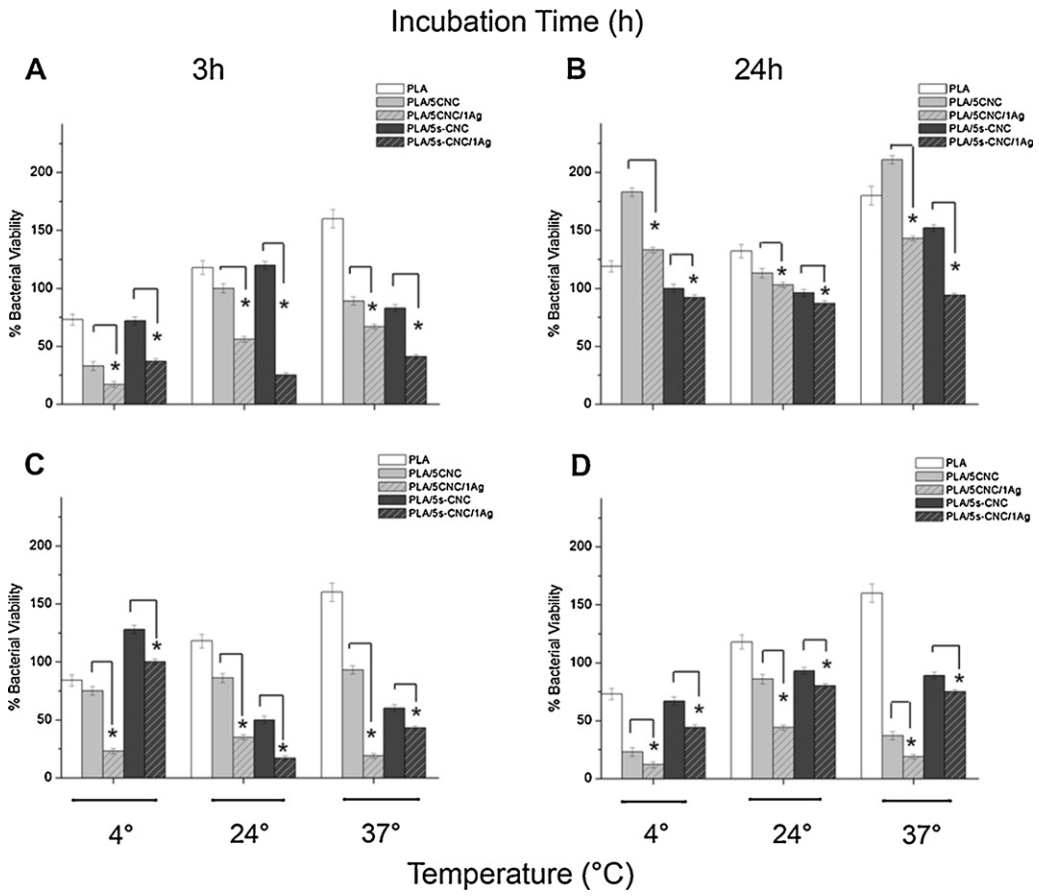

Fig. 9. Antibacterial properties of new multifunctional PLA composites. *S. aureus* 8325-4 (A and B) and *E. coli* RB (C and D) cells were seeded onto PLA and PLA nanocomposite films and incubated for 3 h and 24 h at 4 °C, 24 °C and 37 °C, respectively. Results are expressed on a biomaterial-basis and are presented as an average ± standard deviation ($^{*}p < 0.05$).

Furthermore, we found that the antibacterial activity of the PLA samples containing Ag nanoparticles was greater on *E. coli* than on *S. aureus* cells regardless of the times and temperatures of incubation. In fact, previous studies showed that Ag nanoparticles are more toxic to *E. coli* than to *S. aureus* (Li et al., 2010; Wen-Ru et al., 2011).

For *S. aureus*, the antibacterial activity was still remarkable, regardless of the temperature selected, on PLA/5s-CNC/1Ag at longer incubation time (24 h) considering the greatest percent of bacterial attachment on PLA (Fig. 9b). After 3 h incubation, PLA/5s-CNC/1Ag showed the best performance either at 24 °C and 37 °C (Fig. 9a). On the contrary, for *E. coli* cells, after 24 h incubation time, PLA/5CNC/1Ag showed the best antibacterial activity regardless the temperatures chosen for the experiments (Fig. 9d). Likely, after 3 h incubation, *E. coli* viability on PLA/5CNC/1Ag was significantly reduced at 4 °C and 37 °C; at 24 °C, *E. coli* percent of survivability was reduced on PLA/5s-CNC/1Ag (Fig. 9c).

The reduced antibacterial activity on *S. aureus* may be due to its structural character. Gram-positive and Gram-negative cells differ markedly in their cell walls. Obviously, the peptidoglycan in the cell walls of Gram-positive cells is much thicker than that in the Gram-negative ones. The thicker cell wall of *S. aureus* is of immense practical importance in protecting the cell from penetration of silver ions into the cytoplasm. Once inside the bacterial cell, the Ag^{+} ions are known to interact with thiol groups of the proteins and inactive the enzyme activity (Liau, Read, Pugh, Furr, & Russell, 1997); silver ions turning DNA into a condensed form lead to the damage or even the death of the microorganisms (Feng et al., 2000; Kim et al., 2007). Furthermore, it was found that the silver powder with a particle nanometer distribution in a polymer matrix showed the highest Ag^{+} ion release (Kumar & Munstedt, 2005). The results of the present study suggest that the better dispersion of Ag nanoparticles in the PLA/5s-CNC/1Ag ternary nanocomposites, as already confirmed by morphological, thermal and mechanical analysis, affect positively the interaction of Ag^{+} ions with the bacteria (Kumar & Munstedt, 2005) and this mechanism was found to be more important for *S. aureus* cell respect to *E. coli*, due to different bacteria properties.

In summary, for both bacterial strain tested the antibacterial activity was more evidenced on PLA films containing Ag, and the nanometer dispersion of the silver particles was confirmed as an important factor.

4. Conclusions

Binary and ternary PLA nanocomposite films were prepared by twin-screw extrusion followed by a film formation process combining cellulose nanocrystals and silver nanoparticles. Cellulose nanocrystals were synthesized from MCC by sulphuric acid hydrolysis and the hypothesis to modify crystal surface with surfactant as a means to improve the dispersion of filler in PLA matrix was successfully confirmed. The presence of surfactant on the nanocrystal surface favours the dispersion of the nanocellulose in the PLA matrix and the nucleation effect was remarkably enhanced highlighting the effect of the crystals and of their surface modification on the thermal and mechanical properties of the nanocomposites. A bactericidal effect of nanocomposites on *S. aureus* and *E. coli* was detected suggesting that these systems may offer good

perspectives for food packaging and sanitary applications which requires an antibacterial effect constant over time while further investigation of the expected increase of gas barrier properties, and moisture migration and flavour and aroma control are in progress taking into account the field of application.

Acknowledgments

The authors gratefully acknowledge the financial support from INSTM. We also acknowledge the Analytical Chemistry, Nutrition & Food Sciences Department of the University of Alicante, Spain and in particular Prof. Alfonso Jimènez. L. Visai would like to acknowledge financial support by the International Centre for Studies and Research in Biomedicine (I.C.B.) in Luxembourg, by "Project SAL-45" financed by Regione Lombardia (2010) and by project financed by FONDAZIONE ALMA MATER TICINENSIS (2010).

References

Auras, R., Harte, B. & Selke, S. (2004). An overview of polylactides as packaging materials. *Macromolecular Bioscience*, *4*, 835–864.

Bondeson, D., Mathew, A. & Oksman, K. (2006). Optimization of the isolation of nanocrystals from microcrystalline cellulose by acid hydrolysis. *Cellulose*, *13*(2), 171–180.

Bondeson, D. & Oksman, K. (2007). Dispersion and characteristics of surfactant modified cellulose whiskers nanocomposites. *Composite Interfaces*, *14*, 617–630.

Bondeson, D., Syre, P. & Oksman, K. (2007). *Journal of Biobased Materials and Bioenergy*, *1*, 1.

Bordes, P., Pollet, E. & Avérous, L. (2009). Nano-biocomposites: Biodegradable polyester/nanoclay systems. *Progress in Polymer Science*, *34*, 125–155.

Cavaille, J. Y., Ruiz, M. M., Dufresne, A., Gerard, J. F. & Graillat, C. (2000). Processing and characterization of new thermoset nanocomposites based on cellulose whiskers. *Composite Interfaces*, *7*(2), 117–131.

Colom, X., Carrasco, F., Pages, P. & Canavate, J. (2003). Effects of different treatments on the interface of HDPE/lignocellulosic fiber composites. *Composite Science and Technology*, *63*, 161–169.

Cranston, E. D. & Gray, D. G. (2006). Morphological and optical characterization of polyelectrolyte multilayers incorporating nanocrystalline cellulose. *Biomacromolecules*, *7*, 2522–2530.

Davis, G. & Song, J. H. (2006). Biodegradable packaging based on raw materials from crops and their impact on waste management. *Industrial Crops and Products*, *23*, 147–161.

Dong, X. M., Revol, J. F. & Gray, D. G. (1998). Effect of microcrystallite preparation conditions on the formation of colloid crystals of cellulose. *Cellulose*, *5*(1), 19–32.

Edgar, C. D. & Gray, D. G. (2002). Influence of dextran on the phase behavior of suspensions of cellulose nanocrystals. *Macromolecules*, *35*(19), 7400–7406.

Feng, Q. L., Wu, J., Chen, G. Q., Cui, F. Z., Kim, T. N. & Kim, J. P. (2000). A mechanistic study of the antibacterial effect of silver ions on *Escherichia coli* and *Staphylococcus aureus*. *Journal of Biomedial Materials Research*, *52*(4), 662–668.

Fortunati, E., Armentano, I., Iannoni, A. & Kenny, J. M. (2010). Development and thermal behaviour of ternary PLA matrix composites. *Polymer Degradation and Stability*, *95*, 2200–2206.

Ha, J. U. & Xanthos, M. (2010). Novel modifiers for layered double hydroxides and their effects on the properties of polylactic acid composites. *Applied Clay Science*, *47*, 303–310.

Heux, L., Chauve, G. & Bonini, C. (2000). Nonflocculating and chiral-nematic self-ordering of cellulose microcrystals suspensions in nonpolar solvents. *Langmuir*, *16*(21), 8210–8212.

Kim, J. S., Kuk, E., Yu, K. N., Kim, J., Park, S. J., Lee, H. J., et al. (2007). Antimicrobial effects of silver nanoparticles. *Nanomedicine: Nanotechnology, Biology and Medicine*, *3*, 95–101.

Kim, Y. S., Kim, J. S., Cho, H. S., Rha, D. S., Kim, J. M., Park, J. D., et al. (2008). Twenty-eight-day oral toxicity, genotoxicity, and gender-related tissue distribution of silver nanoparticles in Sprague–Dawley rats. *Inhalation Toxicology*, *20*, 575–583.

Kumar, R. & Munstedt, H. (2005). Silver ion release from antimicrobial polyamide/silver composites. *Biomaterials*, *26*, 2081–2088.

Kvien, I., Tanem, B. S. & Oksman, K. (2005). Characterization of cellulose whiskers and their nanocomposites by atomic force and electron microscopy. *Biomacromolecules*, *6*, 3160–3165.

Li, W. R., Xie, X. B., Shi, Q. S., Zeng, H. Y., Ou-Yang, Y. S. & Chen, Y. B. (2010). Antibacterial activity and mechanism of silver nanoparticles on *Escherichia coli*. *Applied Microbiology and Biotechnology*, *85*, 1115–1122.

Liao, R., Yang, B., Yu, W. & Zhou, C. (2007). Isothermal cold crystallization kinetics of polylactide/nucleating agents. *Journal of Applied Polymer Science*, *104*, 310–317.

Liau, S. Y., Read, D. C., Pugh, W. J., Furr, J. R. & Russell, A. D. (1997). Interaction of silver-nitrate with readily identifiable groups—Relationship to the antibacterial action of silver ions. *Letters in Applied Microbiology*, *25*, 279–283.

Lu, P. & Hsieh, Y. L. (2010). Preparation and properties of cellulose nanocrystals: Rods, spheres, and network. *Carbohydrate Polymers*, *82*, 329–336.

Lunt, J. (1998). Large-scale production, properties and commercial applications of polylactic acid polymers. *Polymer Degradation and Stability*, *59*, 145–151.

Martino, V. P., Ruseckaite, R. A. & Jiménez, A. (2006). Thermal and mechanical characterization of plasticized poly(L-lactide-co-D,L-lactide) films for food packaging. *Journal of Thermal Analysis and Calorimetry*, *86*, 707–712.

Morones, J., Elechiguerra, J., Camacho, A., Holt, K., Kouri, J., Ramirez, J., et al. (2005). The bactericidal effect of silver nanoparticles. *Nanotechnology*, *16*, 2346–2353.

Oksman, K., Mathew, A. P., Bondeson, D. & Kvien, I. (2006). Manufacturing process of cellulose whiskers/polylactic acid nanocomposites. *Composite Science and Technology*, *66*, 2776–2784.

Pei, A., Zhou, Q. & Berglund, L. A. (2010). Functionalized cellulose nanocrystals as biobased nucleation agents in poly(L-lactide) (PLLA)—Crystallization and mechanical property effects. *Composite Science and Technology*, *70*, 815–821.

Petersson, L. & Oksman, K. (2006). Biopolymer based nanocomposites: Comparing layered silicates and microcrystalline cellulose as nanoreinforcement. *Composite Science and Technology*, *66*, 2187–2196.

Petersson, L., Kvien, I. & Oksman, K. (2007). Structure and thermal properties of poly(lactic acid)/cellulose whiskers nanocomposite materials. *Composite Science and Technology*, *67*, 2535–2544.

Quintavalla, S. & Vicini, L. (2002). Antimicrobial food packaging in meat industry. *Meat Science*, *62*, 373–380.

Rai, M., Yadav, A. & Gade, A. (2009). Silver nanoparticles as a new generation of microbials. *Biotechnology Advances*, *27*, 76–83.

Riga, A., Zhang, J. & Collis, J. (2004). Characterization of drawn and undrawn poly-L-lactide films by differential scanning calorimetry. *Journal of Thermal Analysis and Calorimetry*, *75*, 257–268.

Roman, M. & Winter, W. T. (2004). Effect of sulfate groups from sulfuric acid hydrolysis on the thermal degradation behavior of bacterial cellulose. *Biomacromolecules*, *5*, 1671–1677.

Samir, M. A. S. A. & Dufresne, A. (2005). Review of recent research into cellulosic whiskers, their properties and their application in nanocomposite field. *Biomacromolecules*, *6*, 612–626.

Vermeiren, L., Devlieghere, F., van Beest, M., de Kruijf, N. & Debevere, J. (1999). Developments in the active packaging of foods. *Trends in Food Science & Technology*, *10*, 77–86.

Wang, N., Ding, E. & Cheng, R. (2007). Thermal degradation behaviors of spherical cellulose nanocrystals with sulfate groups. *Polymer*, *48*, 3486–3493.

Wen-Ru, L., Xiao-Bao, X., Qing-Shan, S., Shun-Shan, D., You-Sheng, O. & Yi-Ben, C. (2011). Antibacterial effect of silver nanoparticles on *Staphylococcus aureus*. *Biometals*, *24*, 135–141.

Williams, R. L., Doherty, P. J., Vince, D. G., Grashoff, G. J. & Williams, D. F. (1998). The biocompatibility of silver. *Critical Reviews in Biocompatibility*, *5*, 221–243.